

Statistical Analysis of Earthquakes and Tsunami of Makran Subduction Zone (MSZ), and Tsunami Hazard Assessment of Gwadar Coast

Mahmood Sultan* and Khawar Ishfaq Ahmed

Centre for Earthquake Studies, National Centre for Physics, Quaid-e-Azam University, Islamabad, Pakistan

Abstract

Tsunami waves are the most underrated hazard affecting the life near coastal belts. With socio-economic developments in coastal region results in more hazardous from tsunami. The hazard assessment of tsunami is highly vital. The Makran region is exceptional in closure zone of Tethys; it is only segment east of the Mediterranean and west of Andaman arc in which subduction of oceanic lithosphere is still an ongoing process. The objective of present study highlights the seismicity of MSZ. It also describes the statistical analysis of the earthquake events after 1973 for the study area, and possible tsunamigenic effects on Gwadar Coast. Fault plane solutions are also correlated with structural map of the study area and delineated the neo-tectonic features. I also try to determine the tsunami hazard assessment, run-up, inundation, maximum sea surface height and first arrival time of the incident waves and amplitude.

ComMIT is used to calculate tsunamigenic parameters at Gwadar coast. The tsunami hazard assessment describes the possible hazardous incidents in near or far future for the coastal area. The velocity estimation of tsunami waves at Gwadar coast depict that, waves have higher velocities. The impact of the tsunami waves will be more at the inner thin portion (Zone-A) of study area having an average elevation of 2 to 3 meters.

Keywords: Makran subduction zone; Earthquakes; Tsunami; Seismicity; Statistical analysis; Tsunami Hazard assesment

Introduction

The southern side of Pakistan is covered by offshore which is a part of Arabian Sea ranging from 61.50° to 68.20° Longitude. The Pakistan offshore is further subdivided into two parts which are separated by Murray Ridge. The eastern part of the Pakistan offshore is Offshore Indus Basin, while the western part of Pakistan offshore is known as Offshore Makran Basin. It occupies from 57.500 to 67.800 longitude, which merges with the Iranian offshore and ends up at Strait of Hormoz. Makran Subduction Zone (MSZ) is distinctive region due to its abnormal behavior of seismicity and structural complexities due to slow rate of subduction. Subduction was probably initiated during Palaeocene time by Platt et al. and accretion started during Eocene time [1] and accretion started during Eocene time [2].

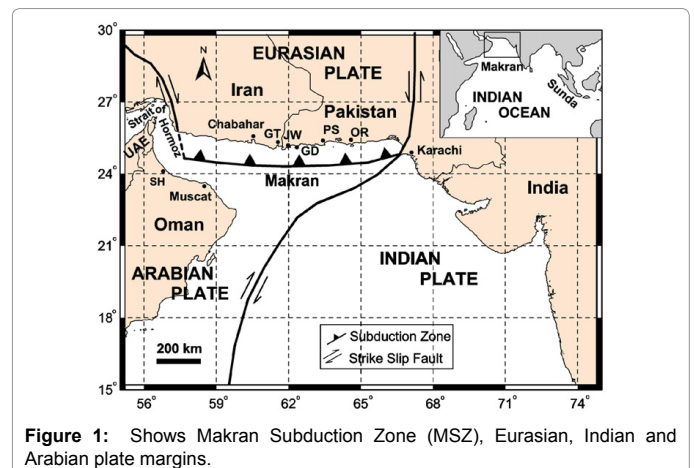
The Makran arc-trench system in Iran and Pakistan is located north of the Gulf of Oman and east of the Zargros Mountains, and straddles the southern margins of the Lut-block and Afghan-block. To the east it is separated from the north-south striking Pakistan fold belts by the Chaman and Ornach-Nal fault systems. The east-west extent of the Makran arc-trench system measures less than 1000 km, and in the north-south direction it widens from about 400 km in the west to about 600 km in the east.

Gwadar

The Gwadar district part of Makran division is situated in the South-West of Pakistan. The geographical coordinates of Gwadar are 25.2°N, 62.19°E making a peninsula like a hammerhead. It has two bays named as Gwadar east bay and Gwadar west bay. The topography of Gwadar is mostly flat but it has two mountains of respectable height known as Koh-e-Batil (137 meter.) and Koh-e-Mehdi (340 meter) (Figure 1).

Tectonic settings

The Makran region is interpreted by a number of workers as a zone of active subduction. Although a bathymetric trench is not observed offshore, most other features of a typical subduction zone can be identified. Sediment deformation, revealed by seismic reflection



profiles off the Makran coast, is similar to that at other compressive plate boundaries [3].

The MSZ forms boundary between the Arabian Plate and Eurasian Plate. [4] stated that the seismicity in the Makran region is consistent with the interpretation of this area as an active subduction zone. According to Quittmeyer and Jacob [4] the raised beaches along the Makran coast confirm the tectonic model of subduction zone along this region.

*Corresponding author: Mahmood Sultan, Centre for Earthquake Studies, National Centre for Physics, Quaid-e-Azam University, Islamabad, Pakistan, Tel: +92-300-634-2456; E-mail: Mahmoodsultan5@gmail.com

Received July 27, 2017; Accepted August 17, 2017; Published August 28, 2017

Citation: Sultan M, Ahmed KI (2017) Statistical Analysis of Earthquakes and Tsunami of Makran Subduction Zone (MSZ), and Tsunami Hazard Assessment of Gwadar Coast. J Earth Sci Clim Change 8: 408. doi: [10.4172/2157-7617.1000408](https://doi.org/10.4172/2157-7617.1000408)

Copyright: © 2017 Sultan M, et al. This is an open-access article distributed under the terms of the Creative Commons Attribution License, which permits unrestricted use, distribution, and reproduction in any medium, provided the original author and source are credited.

Transpressional strike-slip system, the Ornach-Nal fault system, form the eastern boundary of the MSZ. The Minab-Zendan fault system forms the western boundary of the MSZ as a transition zone between the Zagros continental collision and the Makran Oceanic subduction [2]. To the south, Murry ridge delineates parts of the Arabian-Indian boundary.

Recent studies by employing network of 27 GPS stations in Iran and northern Oman reveal that the subduction rate at the MSZ is about 19.5 mm/y^{-1} [5]. Compared to the convergence rate of the other world's subduction zones, MSZ is a relatively slow-moving subduction zone. MSZ is extremely shallow subduction angle [6]. Seismic reflection profile across the MSZ showed that the MSZ includes extremely low dip angle ranging between 2° and 8° [7]. Unlike the other world's subduction zones, there is no trench at the location of the MSZ [7]. As for many subduction zones, active mud volcanoes are present all along the MSZ [8].

Data set

The data set includes the earthquake catalogue, topography and bathymetry data for ComMIT. The earthquake event data is acquired from Pakistan Metrological Department (PMD), (This catalogue is ranging from 1990-2012. This catalogue has been used for interpreting the Seismicity of the area.) and United States Geological Survey (USGS), (This catalogue is ranging from 1973-2012. This catalogue has been used for Statistical Analysis.). The Centroid Moment Tensor has been used for the interpretation of Fault Plane Solutions (FPS).

The Components of Present Study

Seismological behavior of Makran subduction zone (Msz)

The effect of earthquake energy on particular area depends upon several factors, like Magnitude, Lithology of the area, and distance from epicenter, depth of the event and structural strength of that area. Seismicity of any particular region is determined through frequency of several factors such as,

1. Magnitude of earthquakes in particular time
2. Depth of earthquakes in particular time (Shallow focus, Deep focus)
3. Intensity of earthquakes in particular time

Seismicity and earthquake catalogue of MSZ

At MSZ the Arabian plate is being subducted by Eurasian plate. The MSZ shows abnormal behavior of seismicity. Its eastern part is quite active as compared to western part. The historical study illustrates that the eastern part of Makran has many records but the western part exhibited no seismicity [2]. The earthquake catalogue is obtained from preliminary determination of epicenters (PDE) operated by United States Geological Survey (USGS). The catalogue used (1973-2011) containing 177 events shown in Figure 1. The 3.7 Mw is the threshold of the catalogue and the Maximum amplitude in the catalogue is 5.9 Mw.

Historical Background of Seismicity

Seven earthquakes at MSZ are reported by Byrne et al. [2], among which six earthquakes might have ruptured the plate boundary in four parts. He also has concluded that if entire plate motion between Eurasian and Arabian plate happened during events like 1945, the recurrence interval at eastern part for +8 magnitude would be 175 years. Due to lack of data about occurring big events occurrence in western part of

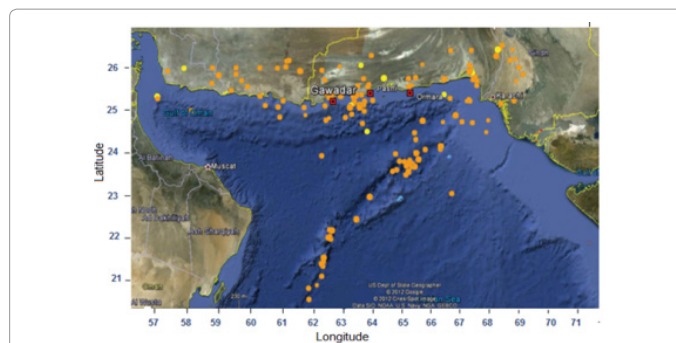


Figure 2: Shows the location of all events present in catalogue.

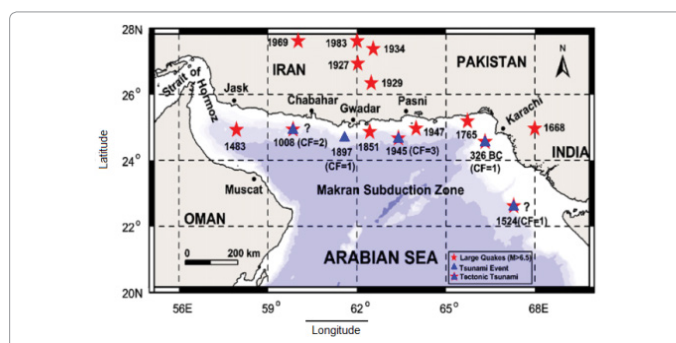


Figure 3: Shows historical earthquake demonstration of eastern and western parts of the MSZ. CF represents confidence factor [9].

MSZ, there is no estimation about the recurrence interval about future earthquakes. The historical earthquakes ≥ 6.5 magnitudes are presented in Figure 2 below.

Earthquake Parameters

The Fault Plane Solutions (FPS) or Focal Mechanisms Solutions and Source Parameters both are instrumental parameters, more sophisticated the instrument then more reliable the information. The basic parameters of an earthquake are magnitude, location, time, and depth of an event. Source parameters can fluctuate from station to station because they are instrumental parameter affected by different orientation, recording devices, staff (trained or untrained), variation of subsurface lithology etc. The local observatories are preferred because the variations are less.

In the MSZ, the earthquake distribution is quite odd, detailed earthquake magnitude study describes that this zone has the Light to Moderate level seismicity as presented in below Figure 3.

These numbers suggest, MSZ is not among the active zones and the recurrence period, for Major or Great events is quite large. The magnitude of 177 events has been plotted. The cluster of the events represents the subsurface structure of the area. The density of the events is high between 24.00 to 26.00 degrees Latitude. The three colors show the level of seismicity in the area. The blue color which has only one event symbolizes the Minor seismicity, while the red color represents the Light seismicity, and the black color depicts the moderate level seismicity.

The graph of 177 events below describes total number of events for a particular earthquake class. This graph in Figure 4 shows that the area has light to moderate level of seismicity, which is not too much hazardous for the Gwadar and nearby coasts. But a major or great earthquake can cause catastrophic effects in the entire region like 1945 great earthquake.

The depth of an earthquake is the precise study of lithology between focus and recorder. The velocity structure of any area is developed by this parameter. These events depict the depth of earthquakes along the major structures. Two ranges of depth have been marked i.e. shallow level (0 to 30 Km) and intermediate level (30 to 70 Km), while no deep earthquake has been reported. The trend is from shallow to intermediate foci of earthquakes as in Figure 5. The event with shallow to intermediate depth and has major to great magnitude range, can cause devastation i.e. the depth of 1945 great earthquake was 27 Km [2] as described by Byrne et al. having magnitude 8.1 Mw. So, the MSZ has the ability to produce the hazardous tsunamis with earthquake of shallow focus and magnitude >7.

Correlation of Source Parameters

The correlation of the source parameters provides us the seismicity pattern of the area and in identification of neotectonic features. The best seismicity pattern can be obtained by interlinking the different parameters.

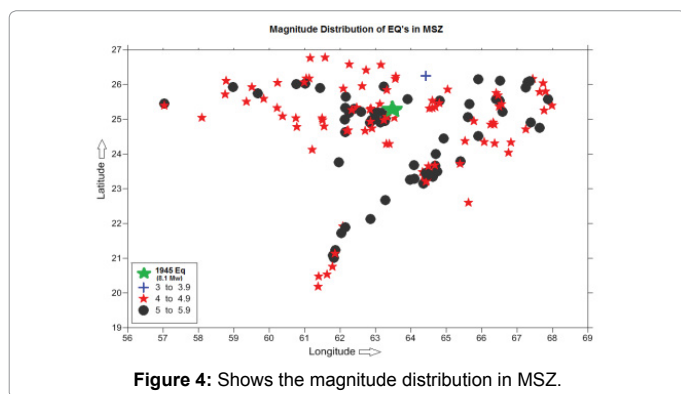


Figure 4: Shows the magnitude distribution in MSZ.

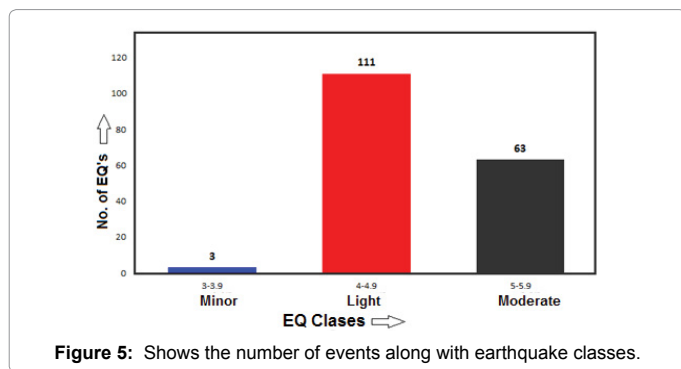


Figure 5: Shows the number of events along with earthquake classes.

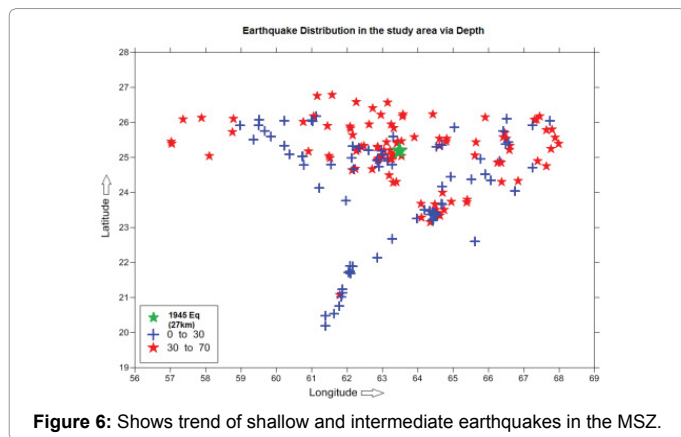


Figure 6: Shows trend of shallow and intermediate earthquakes in the MSZ.

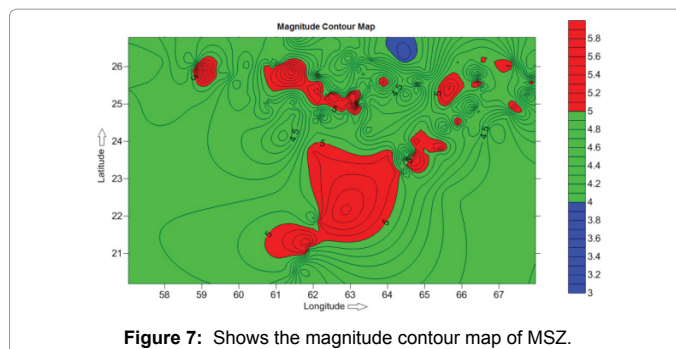


Figure 7: Shows the magnitude contour map of MSZ.

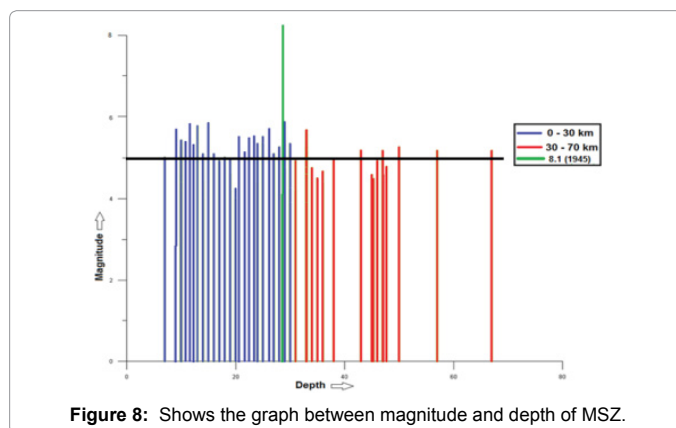


Figure 8: Shows the graph between magnitude and depth of MSZ.

The correlation between magnitude and location is the distribution of magnitude within the region. The cluster of the events at specific places indicates the active zones in the area and is helpful in finding out the causative fault. In MSZ, 177 events are used to depict the seismicity of the region in Figure 6. The central point of the map indicates the active zone with a moderate level of seismicity while green color dominates the map i.e. light seismicity. This fact illustrates that the MSZ is predominantly influenced by light to moderate level seismicity.

While developing correlation between magnitude and depth, the seismicity pattern is produced without incorporating the location, which can be represented in graphical format. The graph depicts the frequency of shallow and deep earthquakes in the study area, which is shown in Figure 7 below. The depth of the 1945 event is also marked in this graph, which lies in the shallow depth events range. The black horizontal line in the graph shows the average magnitude in the MSZ, which lies in moderate level seismicity with shallower depth events.

The correlation between depth and location leads us to find the location, depth, extension, and orientation of the active fault zone, ultimately to hazard assessment. In MSZ, mostly earthquakes are shallow focus with an average depth of 0 to 30 Km, while intermediate events range from 30 to 70 Km. The deepest earthquakes lie east of Gwadar. The cluster of shallow earthquakes lies near the eastern part of Gwadar as shown in the depth distribution map below (Figure 8). There are two events located at Gwadar; these events have intermediate depth, and these can also be noticeable at 25.2 and 62.19 degrees. The map of the area is dominant with shallow to intermediate events, for major or great events, this depth range is unsafe for the nearby coasts.

Intensity Map of the Makran Subduction Zone

The intensity of an earthquake can be different at different locations; this differentiation is caused by the subsurface lithology,

epicentral distance, cultural structures, population density and tectonics of the area. For intensity map we used Modified Mercalli Scale (MMI), to analyze the seismic hazard assessment of MSZ. The intensity is calculated by comparing the magnitudes with MMI scale. The magnitude data which is available is in moment magnitude scale, at first these all magnitudes are converted to richter magnitude scale by using following equation,

The equation (a) is used to determine surface wave magnitude (M_s) by using moment magnitude (M_w), and equation (b) is used to determine Richter magnitude scale (M_l) by using equation (a).

$$M_s = (M_w - 2.07) / 0.67 \quad (a)$$

$$M_l = (0.58(M_s) + 1.20) / 0.82 \quad (b)$$

Where ' M_s ' represents surface wave magnitude, ' M_w ' represents moment magnitude and ' M_l ' represents the Richter magnitude.

The map in Figure 9 depicts moderate to strong level of tremors, while the violent tremors are not common.

Fault Plane Solutions (FPS) or Focal Mechanisms Solutions

FPS is the outcome of earthquake waves which are recorded by several seismometers. The result of these focal mechanisms solutions is the beach ball diagram. The 38 beach ball diagrams are prepared to interpret the orientation and nature of faulting in the area.

Parameters

These include the source parameters and fault plane parameters, these are as follows:

Date

The oldest fault plane solution in the area is FPS-01 which has the date 29 May 1977 earthquake while the latest is FPS-38, has a date of 04 January 2012.

Location

Fault plane solutions cover the entire MSZ, some northern part of Murray Ridge, Oranch-Nal fault at east and Zendan-Minab fault at west. This all area lies between Latitude 20° to 28° and Longitude 56° to 69°.

Depth

The area is dominant with shallow to intermediate events. The FPS-31 has maximum depth of 84 Km's, while the shallowest depth is owned by two FPS which are FPS-01 and FPS-10 of depth 10 Km's. The FPSs of offshore have shallow depths.

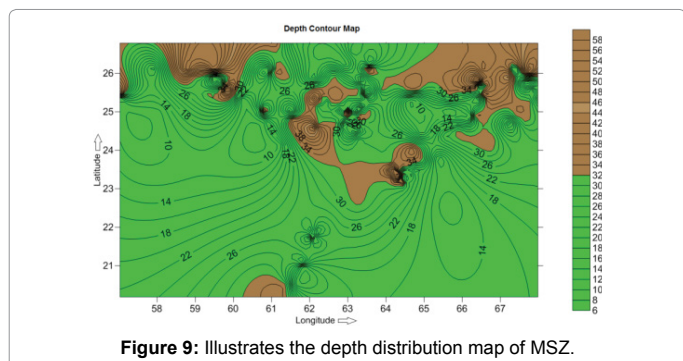


Figure 9: Illustrates the depth distribution map of MSZ.

Magnitude

The MSZ is mainly subjective to light to moderate level of seismicity. The maximum magnitude is possessed by FPS-14 which is 6.1 Mw.

Fault plane

The flat or planar surface of the fault along with movement take place is known as fault plane.

1. Auxiliary plane: This line is perpendicular to the fault plane or it is perpendicular to the plane which describes the earthquake direction.

2. Hypocenter: It is the point of origination of the earthquake on the rupture plane. The epicenter lies directly above to the focus of an earthquake.

Fault Plane Solutions Catalogue

In the present study fault plane solutions are prepared. This data is as below. The abbreviations used are as under in Table 1.

Structural Interpretation of MSZ by Fault Plane Solutions (FPS)

Instrumental seismology is the tool in delineating the inner structure of the earth. Seismically area is light to moderate level active, but the frequency of earthquakes is high in the region. For MSZ, FPSs are plotted on the structural map of the area. Most of the FPSs correlate themselves to the faults present in structural map as shown in Figure 10 below.

Generally, the area is subjected to have a compressional regime due to subduction but it is also associated with transform movement at eastern side. This transform component is quite prominent as illustrated by FPS on the structural map. The presence of several kind forces results the structure complexity and generation of transpressional features.

The FPS of 1945 historic earthquake is plotted on the structural map. FPS of the event shows thrust fault with some strike slip component. Most of the FPSs align themselves with the Murray ridge confirming the strike slip movement in the ridge. The FPS at Oranch-Nal fault also confirms its strike slip behavior, but one FPS shows pure thrusting which may be created due to the MSZ. Moreover, the FPSs at western side of MSZ also align themselves to Zendan-Minab fault. Some localized extensional regime features can also be seen by FPS but are minor.

At western side of the Oranch-Nal fault the FPS have large closure. This closure is generated either by the Oranch-Nal fault or by some active blind fault.

Statistical Analysis

The earthquake catalogue used in this study is obtained from Preliminary Determination of Epicenters (PDE) operated by United States Geological Survey (USGS).

The statistical analysis shows the comparison as well as upcoming possible events of the area. The 'Gutenberg-Richter Law' (GR Law) is applied in this case study.

The basic parameters for GR law are as follows:

Catalogue Analysis

The source parameters of earthquake events of MSZ are as,

1. Date: 1st January 1973 to 31st May 2012.

| S.No | Lat | Long | Time (GMT) | Date (D/M/Y) | Depth (Km) | Mw | FP | | | AP | | | HD | CT - HT |
|------|-------|-------|------------|--------------|------------|-----|-----|----|------|-----|----|------|-----|---------|
| | | | | | | | St | D | SI | St | D | SI | | |
| 1 | 23.07 | 64.47 | 02:22:3.5 | 29/5/1977 | 10 | 5.1 | 135 | 50 | -39 | 252 | 61 | -133 | 1.4 | -0.3 |
| 2 | 23.80 | 65.72 | 01:56:15 | 24/05/1978 | 30 | 5.3 | 110 | 40 | -80 | 277 | 50 | -98 | 1.7 | 4.8 |
| 3 | 26.75 | 61.23 | 01:26:9.4 | 10/01/1979 | 15 | 6 | 338 | 62 | -152 | 234 | 65 | -31 | 3.7 | 0.4 |
| 4 | 26.99 | 60.27 | 02:45:57.9 | 01/1/1980 | 64.1 | 5.4 | 208 | 8 | -178 | 118 | 88 | -10 | 2.1 | 3.9 |
| 5 | 27.73 | 64.33 | 07:04:46.9 | 28/04/1980 | 43 | 5.5 | 39 | 17 | -119 | 249 | 75 | -82 | 2 | 5.2 |
| 6 | 26.28 | 57.21 | 15:06:27.7 | 07/03/1983 | 33 | 5.9 | 05 | 42 | 172 | 101 | 85 | 48 | 3.7 | 0.2 |
| 7 | 27.94 | 62.44 | 10:59:2.9 | 18/04/1983 | 51.3 | 6.7 | 81 | 43 | -68 | 231 | 51 | -109 | 9.3 | 15 |
| 8 | 27.62 | 65.29 | 14:08:20.8 | 18/01/1984 | 15 | 5.6 | 349 | 50 | -13 | 88 | 80 | -139 | 2.4 | -1.0 |
| 9 | 26.96 | 66.45 | 03:19:41. | 02/10/1984 | 12.6 | 5.3 | 191 | 76 | 00 | 281 | 90 | -166 | 1.6 | -3.0 |
| 10 | 20.91 | 62.44 | 21:27:43.1 | 07/4/1985 | 10 | 5.3 | 206 | 90 | 180 | 296 | 90 | 00 | 1.9 | 6.4 |
| 11 | 23.27 | 64.48 | 14:32:16.6 | 19/03/1987 | 35.7 | 5 | 35 | 45 | -138 | 272 | 62 | -54 | 1.2 | -2.4 |
| 12 | 27.91 | 57.25 | 06:42:9.4 | 2/04/1989 | 42.8 | 5.3 | 242 | 24 | 81 | 72 | 66 | 94 | 1.7 | 4.9 |
| 13 | 25.59 | 58.86 | 12:59:37.1 | 07/12/1989 | 15 | 5.9 | 142 | 37 | 103 | 305 | 54 | 80 | 3.5 | 4.5 |
| 14 | 26.75 | 65.25 | 04:51:44.8 | 17/06/1990 | 15 | 6.1 | 210 | 63 | 15 | 114 | 77 | 153 | 4.3 | -1.3 |
| 15 | 27.34 | 65.62 | 17:17:49.3 | 17/06/1990 | 15 | 5.5 | 115 | 56 | 173 | 209 | 85 | 34 | 2.2 | 6.9 |
| 16 | 27.44 | 65.81 | 06:54: 2.3 | 26/07/1990 | 15 | 5.9 | 209 | 63 | 02 | 118 | 88 | 153 | 4.0 | 3.1 |
| 17 | 26.93 | 65.80 | 0:50:39.3 | 14/08/1990 | 15 | 5.5 | 287 | 71 | -170 | 194 | 80 | -19 | 2.1 | 0.5 |
| 18 | 27.55 | 66.23 | 19:33:20.8 | 08/09/1990 | 15 | 5.5 | 197 | 75 | 12 | 104 | 78 | 165 | 2.4 | 1.2 |
| 19 | 25.08 | 62.94 | 14:22:39.2 | 7/12/1991 | 15 | 5.6 | 309 | 08 | 133 | 85 | 84 | 85 | 2.2 | 7.2 |
| 20 | 26.90 | 67.49 | 22:08:0.1 | 21/01/1992 | 15 | 5.4 | 15 | 44 | 75 | 216 | 48 | 104 | 2.4 | 1.3 |
| 21 | 24.25 | 62.88 | 5:22: 2.7 | 30/01/1992 | 15 | 5.8 | 29 | 10 | 126 | 82 | 82 | 84 | 3.3 | 1.3 |
| 22 | 26.75 | 67.36 | 10:17:45.1 | 28/03/1992 | 15 | 4.9 | 03 | 33 | 91 | 182 | 57 | 89 | 1.3 | 3.1 |
| 23 | 27.47 | 65.97 | 07:07:27.6 | 24/04/1992 | 15 | 6 | 102 | 60 | 156 | 205 | 69 | 32 | 4.3 | 2.5 |
| 24 | 25.68 | 61.43 | 12:31:43.0 | 17/12/1992 | 37 | 5.7 | 08 | 54 | 142 | 123 | 6 | 43 | 1.7 | 3.7 |
| 25 | 26.59 | 67.42 | 08:45:44.2 | 28/12/1992 | 33 | 5.1 | 173 | 33 | 32 | 56 | 73 | 119 | 1.0 | 2.7 |
| 26 | 24.31 | 64.99 | 12:31:43.0 | 07/11/2006 | 22.9 | 5 | 137 | 61 | 09 | 43 | 82 | 150 | 0.8 | 1.4 |
| 27 | 22.50 | 63.43 | 09:36:30.0 | 16/11/2006 | 23.4 | 5.3 | 341 | 38 | -33 | 98 | 70 | -123 | 1.1 | 3.2 |
| 28 | 23.22 | 64.36 | 22:40:26.5 | 25/12/2008 | 12 | 5.8 | 215 | 50 | -146 | 101 | 65 | -46 | 2 | 2.9 |
| 29 | 26.98 | 66.37 | 08:36:49.0 | 02/02/2009 | 21.3 | 5.1 | 189 | 81 | -6 | 280 | 84 | -171 | 0.9 | -2.0 |
| 30 | 25.84 | 67.42 | 23:14:48.9 | 17/03/2009 | 12 | 5 | 214 | 45 | 106 | 12 | 47 | 75 | 0.8 | 1.6 |
| 31 | 27.64 | 61.37 | 10:4:28.9 | 30/04/2009 | 84.7 | 5.2 | 21 | 35 | -167 | 280 | 83 | -56 | 1.0 | 2.0 |
| 32 | 25.16 | 57.03 | 22:44:1.5 | 07/05/2009 | 25.2 | 5.1 | 227 | 26 | 82 | 56 | 64 | 94 | 0.8 | -2.9 |
| 33 | 21.67 | 62.00 | 04:12:53.4 | 17/06/2009 | 28.7 | 5.0 | 201 | 18 | 137 | 333 | 77 | 76 | .8 | 1.6 |
| 34 | 27.87 | 66.04 | 16:59:17.7 | 05/06/2010 | 22.3 | 5.0 | 196 | 83 | 06 | 105 | 84 | 173 | 0.8 | 1.7 |
| 35 | 27.75 | 57.12 | 13:49:12.1 | 10/11/2010 | 27.8 | 4.9 | 255 | 36 | 94 | 70 | 54 | 87 | 0.7 | 3.4 |
| 36 | 27.71 | 57.56 | 01:05:29.1 | 15/06/2011 | 41.4 | 5.4 | 333 | 15 | 157 | 79 | 74 | 47 | 1.3 | -1.6 |
| 37 | 27.56 | 64.99 | 00:53:26.6 | 10/08/2011 | 58.5 | 5.8 | 11 | 72 | -163 | 276 | 74 | -19 | 1.9 | 1.9 |
| 38 | 26.61 | 66.05 | 16:51:46.1 | 04/01/2012 | 15.1 | 4.9 | 93 | 64 | -15 | 353 | 70 | -28 | 0.7 | 1.8 |

Lat: Latitude; Long: Longitude, FP: Fault Plane, AP: Auxiliary Plane, St: Strike, D: Dip, SI: Slip, HD: Half Duration, CT: Centroid Time, HT: Hypocenter Time.

Table 1: Presenting of FPS catalog.

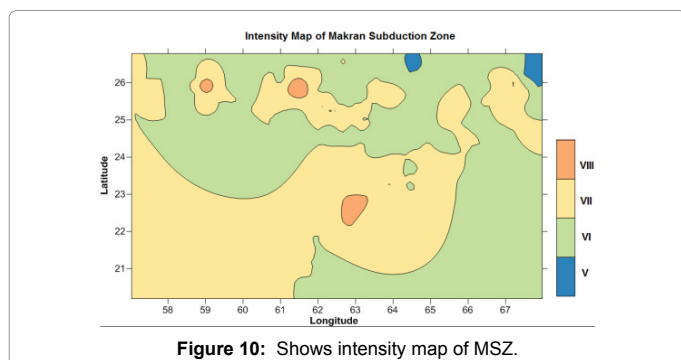


Figure 10: Shows intensity map of MSZ.

2. Location: Latitude=16.000 N-30.000 N

1. Longitude=55.000 E-70.000 E

3. Depth: Shallowest event=0 Km

1. Deepest event=183 Km

4. Magnitude: Minimum magnitude (Threshold)=3.6 Mw

1. Maximum magnitude (Mmax)=7.2 Mw

Frequency Magnitude Distribution

The earthquakes are helpful to crust for releasing its seismic energy which is generated by subsurface stresses and these stresses are accumulated mostly at plate's margin. The "Self Organized Criticality (SOC)" is a technique which suggests that earthquakes organize themselves. The SOC concept then implies that earthquakes in turn organize the crust both at the spatial and temporal levels.

This distribution is plotted between magnitude and number of events carried by each magnitude on a logarithmic scale. In the Figure 11 below the events are approximately following SOC with a b-value of 0.82. This depicts that the area has mostly moderate earthquakes with a few large magnitudes.

Cumulative Number Graph of Earthquakes

The graph prepared by cumulative number of earthquakes and

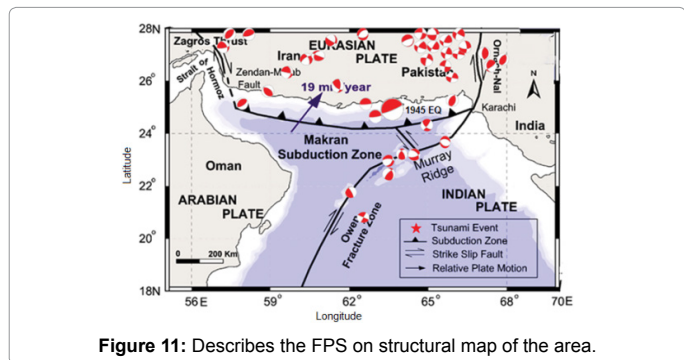


Figure 11: Describes the FPS on structural map of the area.

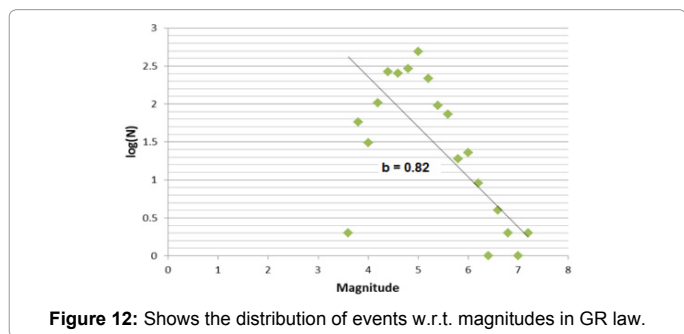


Figure 12: Shows the distribution of events w.r.t. magnitudes in GR law.

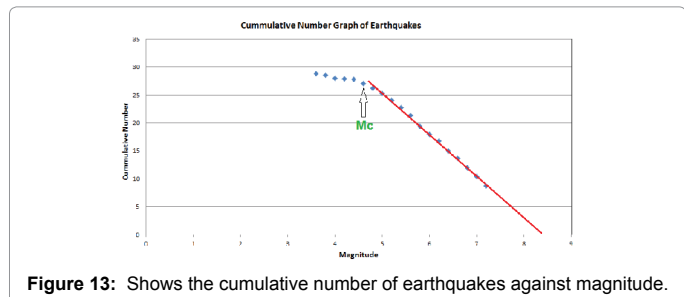


Figure 13: Shows the cumulative number of earthquakes against magnitude.

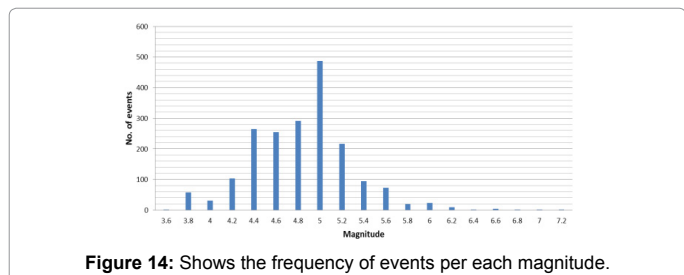


Figure 14: Shows the frequency of events per each magnitude.

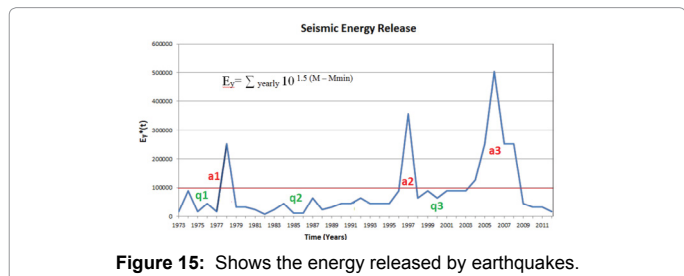


Figure 15: Shows the energy released by earthquakes.

magnitude is as in Figure 12 below. The earthquakes of MSZ present the linear behavior. We can also see the level of completeness. The completeness Magnitude (M_c) is calculated 4.6.

Frequency of the Earthquakes for Whole Catalog

The frequency graph is important for the catalog analysis, on its basis, we specify the magnitude interval that can be used for our statistical study. This graph is plotted between number of events per each magnitude as shown in Figure 13 below. From the graph, it is interpreted that the 0.2 magnitude interval should be used in the study and the common magnitude is around 5 which have the maximum numbers in the catalog.

Calculation of Released Seismic Energy

The released seismic energy E by an earthquake is calculated from magnitude by following formula,

$$E = 10^{d(M-M_{min})} \quad (c)$$

Where E represents released seismic energy, d is Constant which is 1.5 M is magnitude and M_{min} is minimum magnitude of the catalog.

Periods of high seismic activity are characterized by energy rates with an increasing trend in time. It can be observed from the Figure 14 below, there are three times periods of activity after 1973. These three periods are marked by a1, a2 and a3. The seismicity active periods are between 1977-1979 (a1), 1995-1999 (a2) and 2008-2009 (a3). Three periods of quiescence are also marked 1973-1977 (q1), 1979-1996 (q2) and 1998-2004 (q3).

Time Variation of b-Value

The time variations of the b-value in the Gutenberg-Richter law are also dependable over the energy release from event. The b-value is calculated for every three-year interval time and plotted against the time (years). Figure 15 below shows that b-value decreases progressively from 0.8 to 0.4 before 1982. It follows some linear trend upto 1991, then increasing trend and at the level of 0.8 it again become linear upto 2012. The periods of seismic activity are marked by 1977-1979, 1995-1999 and 2008-2009.

Tsunami Hazard Assessment of Gwadar Coast

According to Clague et al. tsunami hazard is normally evaluated by the maximum wave run-up, which can be measured as either the elevation reached by the water, or the horizontal distance the wave floods inland.

1945 Historic Tsunami

Most deadly tsunami in Arabian Sea Occurred at 21:56 UTC, on November 28, 1945. This Tsunami wave generated from a great earthquake of M_w 8.0 located at 25.204° N 63.420° E in the Northern Arabian Sea, about 100 km south of Karachi and about 87 km SSW of Churi (Baluchistan), Pakistan (Pararas-Carayannis 2006). More than 4,000 people were killed by both the earthquake and eruption of mud volcano, a few kilometers off the Makran coast, which is feature of South-West Pakistan, the four small Islands emerged. The Tsunami wave reached a height of 12 m, caused great damage to the entire coastal region (Pararas-Carayannis). The tsunami was also recorded at Muscat and Gawader. This is the only event in Makran subduction zone for which the instrumental data is available such as data about the magnitude of earthquake and run-up values at different coasts [9].

Calculation of Tsunami Potential of Gwadar Coast

The tsunami modeling assists us to map out the historical and upcoming possible disasters. The detailed research on this modeling technique has been carried out after the 2004 Sumatra tsunami, in which every aspect of tsunami progression was studied (www.nctr.pmel.noaa.gov). In present study, the ComMIT software has been used for the estimation of tsunamigenic parameters. The tsunami simulations are executed at MSZ to calculate the result of tsunami waves at Gwadar coast. The MSZ is tsunamigenic, many tsunamis are reported here from which the 1945 was the most destructive and from the future perspective this zone have the potential of generating huge tsunami waves. As Gwadar is an important coast and it is not too far from MSZ, so any 7.5 M_w event can cause destructive results.

The objective of this modeling is to compute the arrival time of first wave hitting the coast and maximum Sea Surface Height (SSH), run-up, inundation and intensity at Gwadar coast. The maximum significance of ComMIT can be obtained by using the good set of values, which are set usually high so that the maximum damage can be calculated. From this calculated damage, the safety levels can be enhanced at the coast. For performing the tsunami hazard study six magnitudes have been used and the epicenters of all these events are placed at MSZ. The applied magnitudes are 7 M_w , 7.3 M_w , 7.5 M_w , 7.7 M_w , 8 M_w , 8.3 M_w and 8.5 M_w , and all the resulting tsunami parameters are determined.

Community Model Interface for Tsunami (ComMIT)

ComMIT gives us first arrival wave time, sea surface height, inundation and run-up. From these parameters, we calculate the intensity of a region. This software works with MOST 'Method of Splitting Tsunami' by Titov and Gonzales and Titov and Synolakis. Elastic deformation model is used by most, at first the model is initialized then the impact of two-dimensional water waves is calculated at the coast.

The input parameters for ComMIT are as follows:

Source parameters selection

The source parameters are the fundamental elements of the tsunami simulation. These are magnitude, depth, location, dip and rupture data of causative fault. In ComMIT Modeling the magnitude varies but the other source parameters are fixed. So, for the six magnitudes there are six models.

1. The magnitudes are 7 M_w , 7.3 M_w , 7.5 M_w , 7.7 M_w , 8 M_w , 8.3 M_w and 8.5 M_w .
2. The location of epicenter is (24.34° 62.00°).
3. The depth of the fault plane is 8 Km.
4. The rupture length is assumed 300 Km.
5. The dip of the fault is 12°.

Grids selection

The grids selection is a critical process. Two types of grids are selected in this tsunami model. These are as follows:

Model grids: In ComMIT three grids were selected for the calculation of tsunami wave's impact on the onshore. These grids are described as A, B and C, and their possible area coverage is 1 arc minute (~1800 m), 6 arc seconds (~180 m) and 2 arc seconds (60 m) respectively. The Figure 16 below shows orientation and location of the three grids.

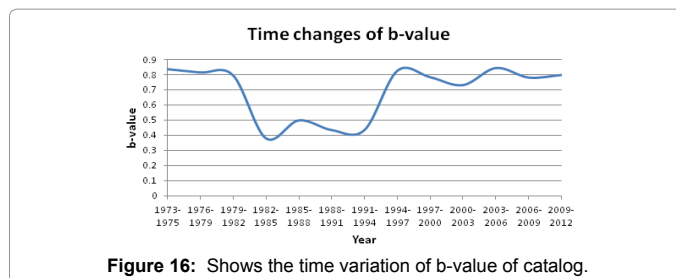


Figure 16: Shows the time variation of b-value of catalog.

| Variables | Units |
|----------------|------------|
| Latitude | 24.724411° |
| Longitude | 63.016786° |
| Strike | 276 |
| Dip | 3.0 |
| Depth of fault | 7.62 Km |
| Length | 100 Km |
| Width | 50 Km |
| Rake | 90 Degrees |

Table 2: Details of source point grids.

The properties of these grids,

1. The Grid A encloses Grid B, while Grid B surrounds the Grid C.
2. These grids must contain both land and sea area.
3. The progression of tsunami waves is calculated by Grid A in open sea, that's why it has a low data resolution.

This low resolution is due to the poor bathymetry and topography data.

4. The Grid B covers some area of open ocean and some shallow region of Gwadar coast, this results a moderate resolution. The resolution of data is moderate because this grid has shallower depth than Grid A. Here software has good control on bathymetry and topography data.

5. The Grid C is the most important grid which computes the tsunami hazard factors like inundation and run-up of Gwadar coast. This grid has high resolution and it covers the entire coast. The control on bathymetry and topography data is extremely perfect.

Source point grids: The source point selection of any area is very important parameter. These describe that how the energy will be dispersed in the area after the earthquake. These grids are automatically generated when the location and magnitude values are loaded in ComMIT. The details of source point grids are presented in Table 2 below.

Along the MSZ there are series of these grids. Twelve green boxes are selected which describe the earthquake source points along the MSZ. These are presented as below in Figure 17.

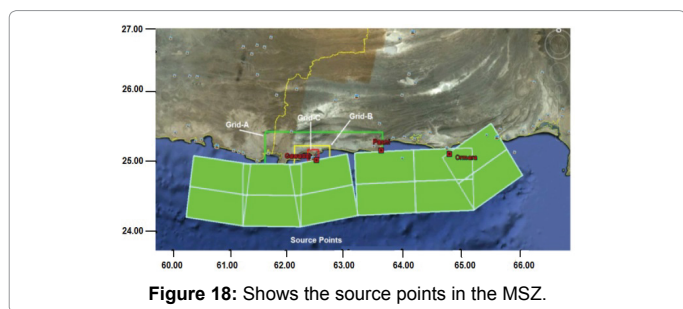
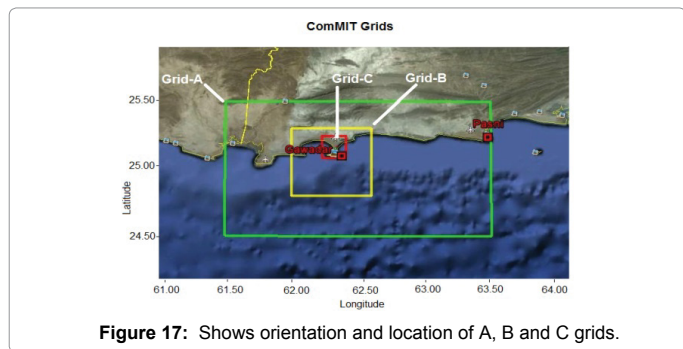
Selection of bathymetric and topographic data

Grids selection is important step. Next step is bathymetric and topographic data. Data is acquired from ETOPO2 (National Geophysical Data set) from the source (<http://www.nctr.pmel.noaa.gov/grid>). The implication of topography and ocean bathymetry on the grids is different. In Figure 18 the Grid A comprises mostly the deep sea, the impact of topography and ocean bathymetry is minimum in deep ocean, this is the reason tsunami waves are not prominent in deep ocean. The Grid B and Grid C are shallower than Grid A, so these are affected by the topography and ocean bathymetry. Shallow depth increases the amplitude of the tsunami waves.

ComMIT Results

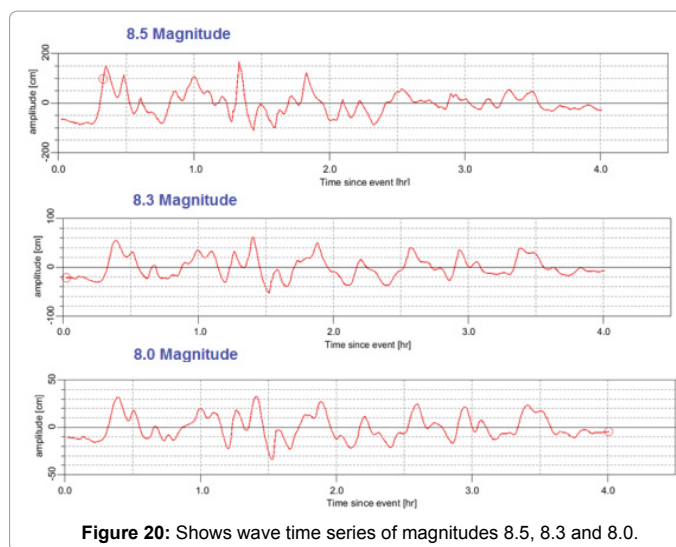
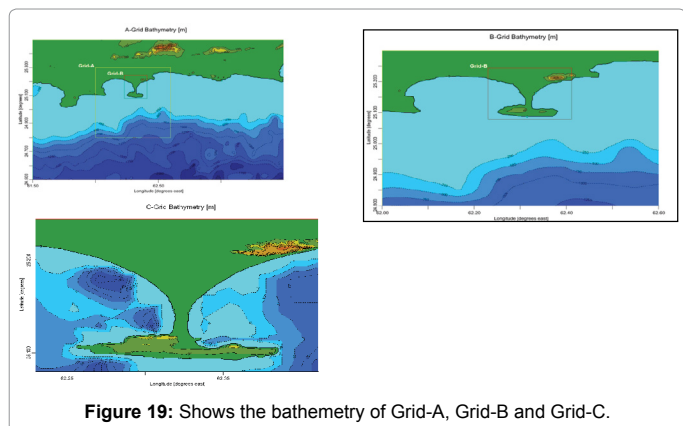
After selecting the input parameters, the model is run for six magnitudes (7 M_w , 7.3 M_w , 7.5 M_w , 7.7 M_w , 8 M_w , 8.3 M_w and 8.5 M_w). The MOST model is used in ComMIT software. This model has 200 steps for 6 hours with step time of 2 seconds. The first arrival wave time, sea surface height, inundation and run-up of tsunami waves were obtained at Gwadar coast. The results are below in Table 3 and Figures 19 and 20.

The detail examination of tsunami waves can take minimum 28



| Magnitude (M_w) | First wave arrival time (mint) | Inundation (m) | Run-up (m) | Max. SSH (m) | Intensity |
|---------------------|--------------------------------|----------------|------------|--------------|-----------|
| 7 | 28 | 0 | 0.0 | 0.01 | 0.3 |
| 7.5 | 27 | 91 | 3.35 | 0.088 | 1.2 |
| 7.7 | 25 | 160 | 6.10 | 0.13 | 1.4 |
| 8.0 | 23 | 205 | 7.01 | 0.34 | 1.8 |
| 8.3 | 22 | 651 | 7.62 | 0.55 | 2.0 |
| 8.5 | 20 | 850 | 9.14 | 1.90 | 2.5 |
| 8.1 (1945 EQ) | 28 | 994 | 8.1 | 0.80 | 2.2 |

Table 3: The ComMIT numerical simulation results of Gwadar.



minutes so that the tsunami warning is delivered to public. In case of Gwadar the velocity of tsunami waves is quite high which is 2.6 Km/sec, that's why the fast computation is needed to rescue the public. As comMIT is too slow to compute the quick results, so it is not practical to use it as early warning system.

The comparison of recorded tsunami height of 8.5 magnitude evaluate that the damageable structures in the Gwadar area. The wooden construction can be swept away or destructed easily while some damage to masonry constructions. It is suggested to avoid the constructions of wooden structures, while the concrete structures are recommended for future safety.

The horizontal distance between the end point of the sea water reached and the shoreline is called inundation distance. The factors affecting inundation are slope of the coastal terrain and friction coefficient of land. The inundation values are different at different sights of Gwadar. The maximum inundation at Gwadar is calculated at east bay, and this is right into the Gwadar city. The inundation produced by 8.5 event is hazardous for the port.

Run-up can be measured as maximum vertical height onshore above sea level. The Gwadar has undulating topography and it is situated at higher altitudes as compare to other coasts. The maximum run-up is generated by the 8.5 M_w which is 9.14 meters calculated at east bay of Gwadar. No run-up is produced by 7 magnitude earthquake. Run-up is depending on wave height of the tsunami waves and slope of the coast. The slope of coast and run-up has direct relation. At Gwadar, the tsunami waves have higher velocities which in result produce high run-up. Almost all events have good heights of run-up except, 7.0 magnitude, which don't have any run-up and inundation.

The inundation and run-up are calculated by the maximum wave amplitude maps below.

The SSH of other five events is less than 1 meter. The comparison of this SSH shows that the earthquakes below than 8 M_w can damage only near shore outdoor accessories such as roads, grounds gardens etc.

It is observed that the 8.5 magnitude has the highest intensity 2.6 while other five events have intensity lower than 1. The intensity of other events is less than 1 shown in Figure 21 this intensity can only damage the near shore outdoor accessories such as roads, grounds gardens etc.

Calculation of Tsunami parameters of 1945 earthquake by using ComMIT

28th November, 1945 earthquake was second deleterious tsunami in Indian Ocean. This tsunami event was recorded on instrument for the first time in this region. This was the only event in MSZ for which the data of the magnitude of earthquake and run-up heights in different coasts is recorded [9-15]. The tsunami hazard parameters of 1945 earthquake are as follows:

The source parameters calculated by Byrne et al. [2] are used in this study for the calculation of tsunami hazard parameters of 1945 earthquake are as under, and wave time series map is shown in Figure 22 and maximum amplitude map is shown in Figure 23.

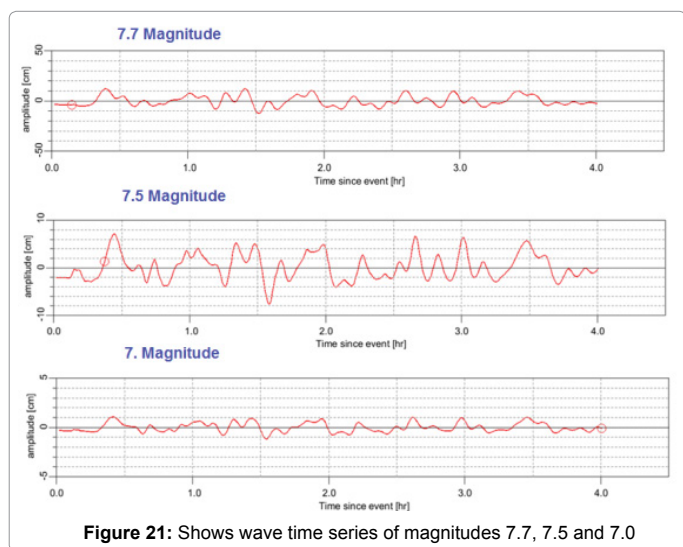


Figure 21: Shows wave time series of magnitudes 7.7, 7.5 and 7.0

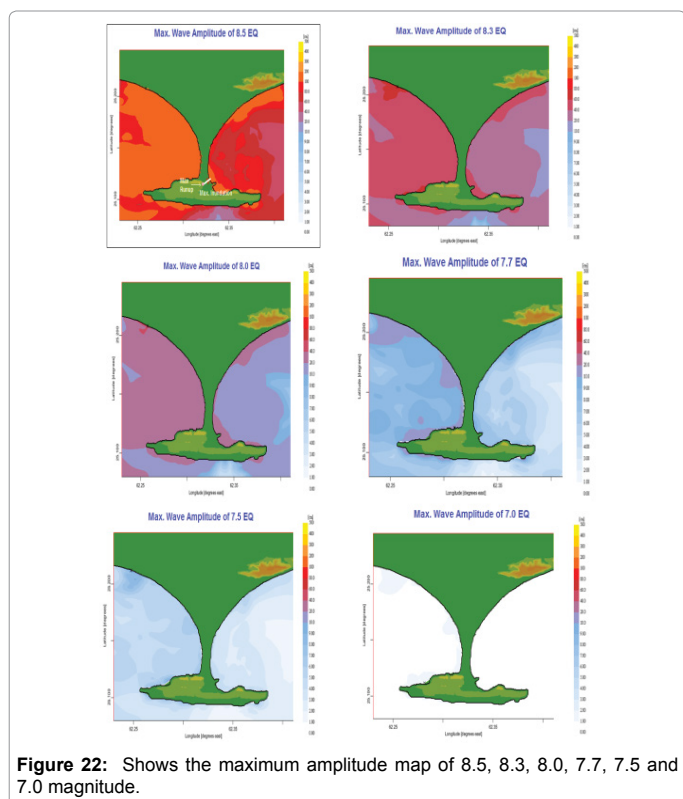


Figure 22: Shows the maximum amplitude map of 8.5, 8.3, 8.0, 7.7, 7.5 and 7.0 magnitude.

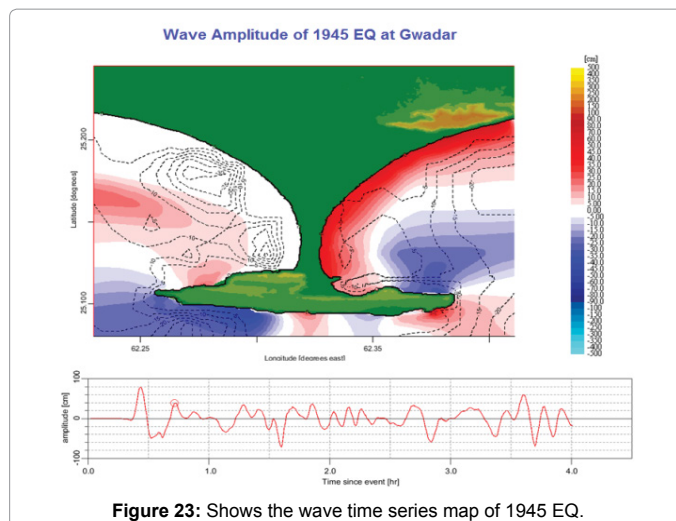


Figure 23: Shows the wave time series map of 1945 EQ.

| Magnitude (Mw) | Time (min) | Time (hr) | Distance (Km) | Velocity (Km/hr) |
|----------------|------------|-----------|---------------|------------------|
| 7 | 28 | 0.467 | 51 | 109.29 |
| 7.5 | 27 | 0.450 | 51 | 113.33 |
| 7.7 | 25 | 0.417 | 51 | 122.40 |
| 8.0 | 23 | 0.383 | 51 | 133.04 |
| 8.3 | 22 | 0.367 | 51 | 139.09 |
| 8.5 | 20 | 0.333 | 51 | 153.00 |
| 8.1(1945 EQ) | 28 | 0.467 | 110 | 235.71 |

Table 4: The velocity behavior of tsunami waves at Gwadar port.

- Location: 25.15, 63.48
- Magnitude: 8.1 Mw
- Rupture length: 100–150 Km
- Rupture width: 100 Km
- Fault slip: 6-7 m
- Dip angle: 7 degree
- Strike angle: 246 degree
- Slip angle: 89 degree
- Depth: 7 Km

Calculation of Tsunami Waves Velocity

For velocity calculation, distance between Gwadar and MSZ is measured 51 Km's, whereas the arrival time of waves is obtained from the first arrival time of tsunami simulation of six events. In deep ocean, the tsunami waves can propagate at higher velocities (800 to 950 Km/hr) and these become much slower as they approach to shore line (40 to 160 Km/hr). The velocity calculation for Gwadar port shows that the maximum velocity of tsunami waves is produced by 8.5 magnitude earthquake. The velocity calculation 1945 historic event have also done. The Table 4 below illustrates the velocity details of seven events.

The velocity analysis at Gwadar port shows that the larger magnitudes take less time to reach the port and respective velocity is high. An increase in velocity is observed as the magnitude of earthquake is increased.

The tsunami waves of the 1945 (8.1 Mw) event reached at Gwadar in 28 minutes. The Gwadar is 110 Km away from the 1945 earthquake

epicenter marked by Byrne et al. [2]. The calculated velocity of this historic event is quite high (235 km/hr). Although this event (1945 EQ, 8.1 Mw) has lower magnitude from other two events (8.5 Mw, 8.3 Mw) but its resulting velocity is too large. This shows that the enormous energy has been released by this historic event and it must have affected the Gwadar.

Calculation of Altitude of Gwadar port for Tsunami Hazard Assessment

The Gwadar has a diverse pattern of elevation. This study is helpful in finding the impact of tsunami waves on different portions of coast. As tsunami waves have strong velocity and high amplitude, that's why their impact is terrible. The tsunami hazard study and altitude study of particular area are significant parameters for avoiding casualties. The scheme of this study is to calculate the altitude at the whole shoreline of Gwadar, and present these values in graphical form (Figure 24).

Gwadar has two bays, named as East bay and West bay. The elevation of these two is same from the sea, it ranges from 0 to 10 feet. These bays are marked as Zone-A in Figure 25 below. The range of elevation in Gwadar is 0 to 262 feet. The front facing portion of Gwadar is marked as Zone-B, it has high altitude as compare to the Zone-A, it ranges from 10 to 262 feet. The detail map of Gwadar is presented below in Figure 26. This altitude indicates that the impact of tsunami waves on this portion is negligible. The Gwadar city lies on Zone-A which has altitude 0 to 10 feet.

The tsunami hazard study of Gwadar area shows that any earthquake larger than 8 magnitude can massively affect the coast. The simulations

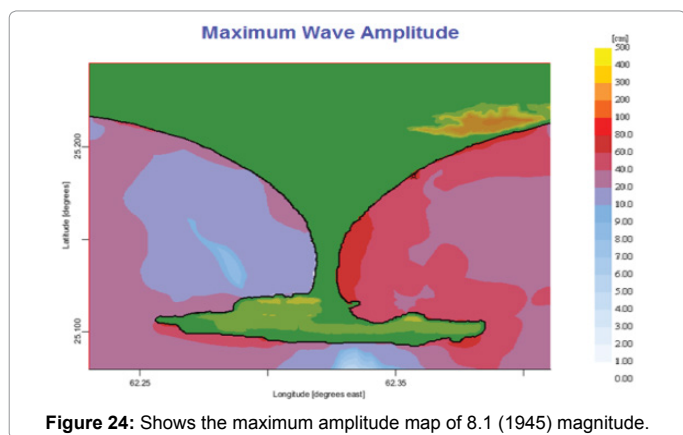


Figure 24: Shows the maximum amplitude map of 8.1 (1945) magnitude.

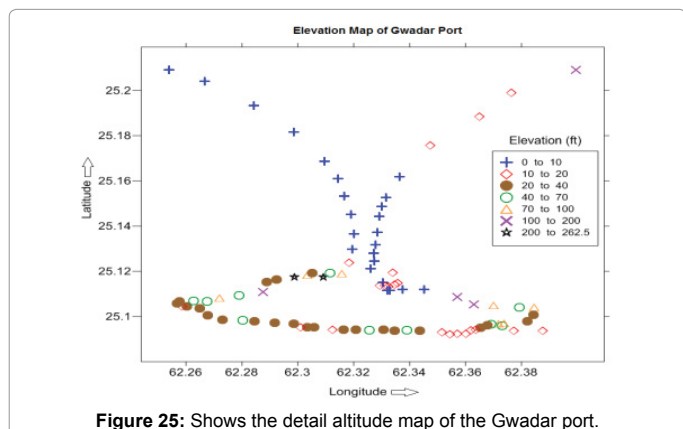


Figure 25: Shows the detail altitude map of the Gwadar port.

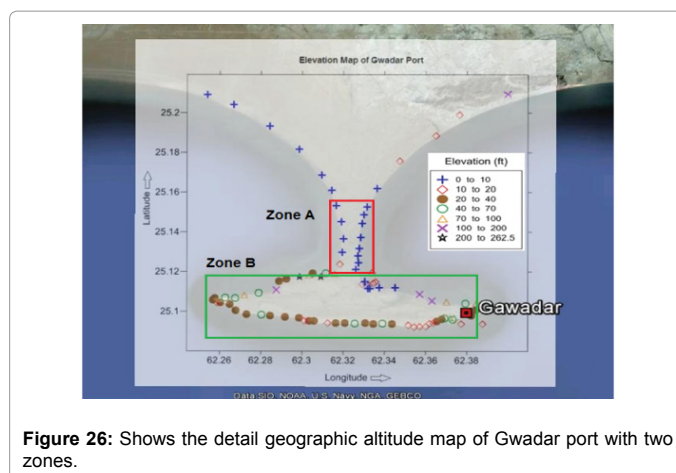


Figure 26: Shows the detail geographic altitude map of Gwadar port with two zones.

of six earthquakes carried out by ComMIT has also maximum results of inundation and run-up heights at Zone-A. The inundation and run-up values of 8, 8.3 and 8.5 magnitude earthquake can cause alarming situation in the region.

The former interpreted results of 1945 earthquake event illustrates that inner region of the port is not safe due to its low altitude. The massive 8.1 Mw earthquake had destroyed the Pasni area in 1945. The calculated results of this event suggest that, at that time Gwadar had faced disastrous effects at eastern bay i.e. Zone-A due to lower altitude and also this portion is inline with the 1945 earthquake epicenter.

The Figure 25 below shows the elevation of Gwadar port with two marked zones. The above map is overlapped with geographic map of the Gwadar. The blue symbols represent the lowest elevation of Gwadar coast, it ranges from 0 to 10 feet. The calculated results by six earthquakes have also maximum influence on Zone-A while the Zone-B is safe due to its high elevation.

Discussion

The MSZ is characterized by shallow seismicity which implies that due to slow convergence at MSZ the earthquake occurring with large magnitude have long recurrence period. The moderate level earthquakes are frequent in the region. Major to great shallow focus event can cause disastrous results in the region. The FPS structural correlation map depicts overall seismic behavior of MSZ which is transpressional. It is controlled by MSZ and transform faulting in the region.

Six event magnitudes are used for the tsunami hazard assessment of Gwadar coast. The magnitudes less than 7.7 Mw show normal values of run-up, inundation and max. sea surface height. The events with magnitude greater than 7.7 Mw show high values of run-up, inundation and max. sea surface height. The maximum values of run-up, inundation and max. sea surface height calculated at Gwadar produced by 8.5 Mw are 9.14 meters, 850 meters and 1.9 meters respectively. The earthquake larger than 8 Mw is alarming for the Gwadar coast.

The calculation of hazard parameters of 1945 earthquake leads us to conclusion that at that time Gwadar also have felt severe damage and flooding. As Gwadar is 110 Km away from the epicenter but Pasni is only 4.7 Km's that's why Pasni was totally swept away. The tsunami waves of this event had targeted the eastern bay of Gwadar, which was head to head to epicenter. While the western bay was quite safe. The results show that this historical event had affected the port tremendously, almost 1 Km inundation and 25 feet run-up must have damaged the Gwadar Zone-A.

The velocity calculations show the bathymetry and topography of the Makran subduction are supportive tools for the generation of high speed waves in the region. The earthquake events greater than 8 magnitudes have high velocities up to 157 Km/hr. The estimated tsunami waves velocity of 1945 earthquake calculated for Gwadar is very high, it is 235 Km/hr. It depicts high strength of tsunami waves in 1945.

Conclusion

The altitude estimation of the Gwadar area leads us to future hazard. The Zone-B has reasonable elevation ranging from 10 to 262 feet, but the average elevation of this portion is 50 feet. Inner thin side marked as Zone-A, is highly sensitive because of low altitude. The calculated run-up and inundation values by ComMIT of six events are also maximum at Zone-A. The Gwadar city is mostly situated on Zone-A so any event greater than 8 Mw can destroy Zone-A easily.

References

1. Platt JP, Leggett JK, Alam S (1988) Slip vectors and fault mechanics in the Makran accretionary wedge, southwest Pakistan. *J Geophysical Res* 93: 7955-7973.
2. Byrne DE, Sykes LR, Davis DM (1992) Great thrust earthquakes and aseismic slip along the plate boundary of the Makran subduction zone. *J Geophys Res* 97: 449-478.
3. White RS, Klitgoro K (1976) Sediment deformation and plate tectonics in the Gulf of Oman. *Earth Planet Sci Lett* 32: 199-209
4. Quittmeyer RC, Jacob KH (1979) Historical and modern seismicity of Pakistan, Afghanistan, northwestern India and southeaster Iran. *BSSA* 69: 773-823
5. Vernant PH, Nilforoushan F, Hatzfeld D, Abbasi MR, Vigny C, et al. (2004) Present-day crustal deformation and plate kinematics in the middle east constrained by GPS measurements in Iran and Northern Oman. *Geophys J International* 157: 381-398.
6. Kopp C, Fruehn J, Flueh ER, Reichert C, Kukowski N, et al. (2000) Structure of the Makran subduction zone from wide angle and reflection seismic data. *Tectonophysics* 329: 171-191
7. Schluter HU, Prexl A, Gaedicke C, Roeser H, Reichert C, et al. (2002) The Makran accretionary wedge: Sediment thicknesses and ages and the origin of mud volcanoes. *Marine Geology* 185: 219-232
8. Wiedicke M, Neben S, Spiess V (2001) Mud volcanoes at the front of the Makran accretionary complex. *Pakistan Marine Geol* 172: 57-73
9. Heidarzadeh M, Pirooza MD, Zakerb NH, Yalciner AH, Mokhtari M, et al. (2008) Historical tsunamis in the Makran subduction zone off the southern coasts of Iran and Pakistan and results of numerical modeling. *Ocean Engineering* 35: 774-786
10. Clague JJ, Munro A, Murty T (2003) Tsunami hazard and risk in Canada. *Natural Hazards* 28: 433-461
11. Richter G (1944) Frequency of earthquakes in California. *Bull Seismol Society America* 34: 185-188
12. Hafeez H (2007) The potential of tsunami generation along Karachi and the Makran coast of Pakistan. *Pakistan J Meteorol* 4: 25-40
13. Pararas G (2006) The potential of tsunami generation along the Makran subduction zone in the Northern Arabian Sea case study: The earthquake and tsunami of November 28, 1945. Presentation at 3rd tsunami symposium of the tsunami society May 23-25, East-West Centre University of Hawaii, Honolulu, Hawaii 24: 358-383
14. Titov VV, Gonzales F (1997) Implementation and testing of the method of splitting tsunami (MOST) model. Technical Memorandum ERL PMEL 112: 11
15. Titov VV, Synolakis CE (1998) Numerical modeling of tidal wave runup. *J Waterway Port Coast Ocean Engineer* 124: 157-171